Journal of
Applied Remote Sensing

RemoteSensing.SPIEDigitalLibrary.org

Drought indices based on MODIS data compared over a maize-growing season in Songliao Plain, China

Yang Song
Shibo Fang
Zaiqiang Yang
Shuanghe Shen

SPIE.

Yang Song, Shibo Fang, Zaiqiang Yang, Shuanghe Shen, "Drought indices based on MODIS data compared over a maize-growing season in Songliao Plain, China," *J. Appl. Remote Sens.* **12**(4), 046003 (2018), doi: 10.1117/1.JRS.12.046003.

Drought indices based on MODIS data compared over a maize-growing season in Songliao Plain, China

Yang Song,[a,b,c] Shibo Fang,[a,b,*] Zaiqiang Yang,[b] and Shuanghe Shen[b]

[a]Chinese Academy of Meteorological Sciences, State Key Laboratory of Severe Weather, Beijing, China

[b]Nanjing University of Information Science and Technology, Collaborative Innovation Center on Forecast and Evaluation of Meteorological Disasters, Nanjing, China

[c]Chinese Academy of Sciences, Northeast Institute of Geography and Agroecology, Changchun, China

Abstract. Many indices based on MODIS data are used to monitor the process of agricultural drought, such as apparent thermal inertia (ATI) and temperature vegetation dryness index (TVDI). Notable differences in performance and geographic predictions exist among these indices. We statistically evaluated the performance of different drought indices for a known drought process in 2014 in the typical rainfed maize region of Songliao Plain, China, using a linear regression model based on the relationships between indices and soil moisture data. Our results show that during the growth season of May to September, the indices performed independently with changing curves, particularly in different phenological periods. By contrast, correlations tended to be higher for ATI than for other indices in the early vegetative growth stage, whereas small differences were detected among the other indices in the late vegetative to late reproductive growth stages. Our results confirm that the TVDI can be the best choice to detect agricultural drought in the study area. © *2018 Society of Photo-Optical Instrumentation Engineers (SPIE)* [DOI: 10.1117/1.JRS.12.046003]

Keywords: agricultural drought indices; spring maize; time series; soil moisture; MODIS.

Paper 180097SS received Feb. 1, 2018; accepted for publication Sep. 18, 2018; published online Oct. 5, 2018.

1 Introduction

Drought is one of the most frequent natural hazards affecting crop growth and causes heavy agricultural damage in China.[1] In 2014, the country was affected by a major drought, with the Songliao Plain, one of main maize-producing areas in China, particularly affected.[2] Rainfall in the whole of Jilin Province between July 1 and August 22 was just 136.9 mm, 49% less than the previous year, causing widespread crop failure.

Timely information on the onset, magnitude, and duration of drought during a crop cycle is crucial for mitigating its impacts. Since vegetation conditions are strongly related to environmental water stress, indices based on remote sensing data can provide valuable information as to the health condition of crops, as well as on monitoring agricultural drought.[3] Various methods based on remote sensing data have been developed to monitor crop drought, collectively referred to as agricultural drought indices. These indices can be helpful for understanding the temporal and spatial variation of agricultural drought and can be useful in devising irrigation strategies, provide early warnings for drought, and accurately estimate crop yield.[4,5]

We classify drought observation indices into three main types: (I) drought indices based on the concept of thermal inertia and the observation of surface temperature change, such as apparent thermal inertia (ATI); (II) drought based on vegetation index, such as normalized difference vegetation index (NDVI), enhanced vegetation index (EVI), and normalized difference moisture index (NDMI), or the vegetation condition index (VCI), which is composed of NDVI, EVI or other vegetation indices, such as VCI_{ndvi} and VCI_{evi}; and (III) drought based

*Address all correspondence to: Shibo Fang, E-mail: Fangshibo@cams.cma.cn

1931-3195/2018/$25.00 © 2018 SPIE

Table 1 Agricultural drought indices and methods based on remote sensing.

Type	Indices	Full name	Reference
I	ATI	Apparent thermal inertia	Price[6]
II	VCI_{ndvi}	Vegetation condition index (NDVI)	Kogan,[7] Tucker,[8,9] Ji[10]
	VCI_{evi}	Vegetation condition index (EVI)	Kogan,[7] Huete[11]
	NDMI	Normalized difference moisture index	Gao,[12] Wilson[13]
III	VSWI	Vegetation supply water index	Carlson[14]
	TVDI	Temperature vegetation dryness index	Sandholt[15]

on a combination of canopy temperature and vegetation index, such as vegetation supply water index (VSWI) and temperature vegetation dryness index (TVDI) (Table 1).

It should be noted that the vegetation cover, which changes across the growth season, is a major factor in agricultural drought monitoring. The three types of drought indices are variably responsive to differences in vegetation cover. ATI, which is based on circadian temperature changes, may be best suited to the period of bare soil or low vegetation cover;[16,17] meanwhile, VCI_{ndvi} and VCI_{evi} detect drought conditions by comparing vegetation index to the previous years' indices, which is more sensitive to high vegetation cover.[18,19] However, VSWI and TVDI rely on vegetation density and canopy temperature, which are sensitive to medium and high vegetation covers.[20,21]

Previous studies give valuable references and ideas for how means of comparison between compare drought indices.[22–24] Bayarjargal et al.[25] used the meteorological drought index (PDSI) instead of soil moisture observations to compare the NOAA-AVHRR derived drought indices in Mongolia, demonstrating differences in each index during the vegetation growth period. To further highlight these differences, we use soil moisture data from automated meteorological stations to assess the performance of MODIS drought indices for agricultural drought monitoring in the Songliao Plain during a whole maize-growing season in 2014. We aimed to (1) clarify trends of the drought indices during the whole crop growth in Songliao plain, China, 2014, and (2) compare their performance in different phenological period.

2 Study Area and Climatic Conditions

The study area is a part of Songliao Plain, situated in the middle and western parts of Jilin Province, Northeastern China, between 42–46°N and 123–127°E (Fig. 1). It is one of the major maize-producing area in the world. The region lies in the warm temperate zone with a semihumid continental monsoon climate of windy and rarely rainy spring, hot and wet summer, cool autumn, and cold dry winter.[26] Winter and summer are longer than spring and autumn. According to statistical data (1971 to 2000), the annual mean temperature is 5°C, mean temperature of the coldest month is −15°C, and mean temperature of the warmest month is 23°C. The annual mean sunshine duration is 2700 h, and the annual precipitation is 522 to 615 mm, of which 60% to 70% falls in summer.[27] Summer maize, the main crop in the study area, is planted in May and harvested in September.[26]

The distribution of precipitation in this region is uneven both in time and space, affected by a continental monsoon climate.[26] Due to these conditions, arid events have occurred frequently. In 2014, a decrease in precipitation led to severe drought in this area.

3 Data and Methodology

3.1 *Data*

In this study, we used MODIS-based products and soil moisture data from automated meteorological stations. MODIS-based products were obtained from the NASA EOSDIS Land Processes

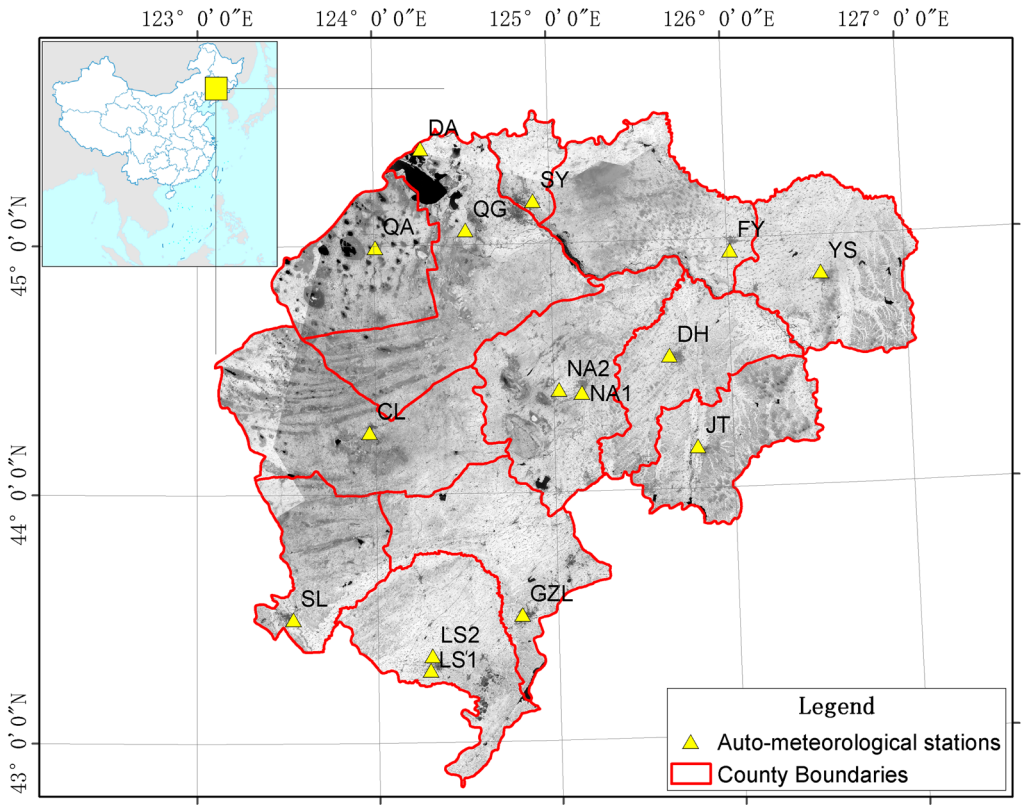

Fig. 1 Location and soil moisture stations of the study area in Songliao Plain.

Distributed Active Archive Center, including the land surface temperature product (MOD11A2: 8-day daytime and nighttime T_s at 1-km spatial resolution) and the surface reflectance product (MOD09A1: 8-day surface reflectance 1 to 7 bands at 500-m spatial resolution). A total of 38 8-day composite products of daytime and nighttime T_s and 190 8-day composite products of surface reflectance between May 9 and September 30 from 2012 to 2016 were used.[28] We calculated agricultural drought indices according to each remote sensing image. Then, ground control points of soil moisture data were derived from 15 automated meteorological stations of CAMS (Chinese Academy of Meteorological Sciences) (Table 2).

3.2 *Drought Indices and Methods*

3.2.1 *Apparent thermal inertia*

The soil moisture retrieval algorithm of ATI is based on the concept of thermal inertia, which is determined by the thermal conductivity of a material. Previous studies have developed the direct use of remote sensing to estimate soil moisture,[29–32] with the ATI per pixel retrieved from images as the ratio of shortwave radiation absorptivity to the land surface temperature difference (ΔLST)

$$\mathrm{ATI} = \frac{1 - A}{\Delta \mathrm{LST}}, \tag{1}$$

where A is the broadband albedo and ΔLST is the diurnal land surface temperature difference between the daytime and nighttime radiometric temperatures of the Terra MODIS. The total visible albedo acquired from MODIS data is regarded as the broadband albedo A in this stud[33]

$$A = 0.331\rho_1 + 0.424\rho_3 + 0.246\rho_4, \tag{2}$$

where ρ_1, ρ_3, and ρ_4 are the reflectance of MODIS band 1, band 3, and band 4, respectively.

Table 2 Automatic meteorological stations in the study area.

Number	Station	Latitude	Longitude	Elevation (m)
1	Nongan (NA1)	44.395	125.16	170.2
2	Nongan (NA2)	44.395	125.157	170.2
3	Lishu (LS1)	43.292	124.29	162
4	Lishu (LS2)	43.35	124.3	160.2
5	Songyuan (SY)	45.171	124.908	147
6	Qianguo (QG)	45.06	124.522	136.2
7	Changling (CL)	44.25	123.967	188.9
8	Fuyu (FY)	44.948	126.018	195
9	Qianan (QA)	44.994	124.009	146.3
10	Dehui (DH)	44.535	125.658	169.9
11	Jiutai (JT)	44.167	125.8	174.5
12	Yushu (YS)	44.85	126.527	196.5
13	Shuangliao (SL)	43.5	123.533	114.9
14	Daan (DA)	45.389	124.274	137.6
15	Gongzhuling (GZL)	43.509	124.8	200.4

3.2.2 *Vegetation condition index: NDVI*

The approach of the normalized difference vegetation index, or NDVI, is based on the fact that well-grown vegetation has a low reflectance in the visible portion of the electromagnetic spectrum and a high reflectance in the NIR due to internal reflectance by the mesophyll spongy tissue of a green leaf.[34] The NDVI can be calculated as

$$\mathrm{NDVI} = \frac{\rho_{\mathrm{NIR}} - \rho_{\mathrm{RED}}}{\rho_{\mathrm{NIR}} + \rho_{\mathrm{RED}}}, \tag{3}$$

where ρ_{NIR} and ρ_{RED} are the NIR and red bands of a sensor system, respectively.

The following $\mathrm{VCI}_{\mathrm{ndvi}}$ equation was applied on the final NDVI database:

$$\mathrm{VCI}_{\mathrm{ndvi}} = \frac{\mathrm{NDVI}_{\mathrm{i}} - \mathrm{NDVI}_{\mathrm{min}}}{\mathrm{NDVI}_{\mathrm{max}} - \mathrm{NDVI}_{\mathrm{min}}}.$$

Here, $\mathrm{NDVI}_{\mathrm{max}}$ and $\mathrm{NDVI}_{\mathrm{min}}$ represent maximum and minimum NDVI, respectively, of each pixel calculated for each 8 days of 5 years from 2012 to 2016, and NDVI_i represents the index of the current 8 days. $\mathrm{VCI}_{\mathrm{ndvi}}$ is measured in a range from 0 to 1. Values below 0.35 indicate severe drought conditions, values between 0.35 and 0.5 indicate drought, and values between 0.5 and 1 indicate normal conditions.[35]

3.2.3 *Vegetation condition index: EVI*

The EVI was developed to optimize the vegetation signal with improved sensitivity in high biomass regions and improved vegetation monitoring through a decoupling of the canopy background signal and a reduction in atmosphere influences. It can be calculated as

$$\mathrm{EVI} = 2.5\frac{\rho_{\mathrm{NIR}} - \rho_{\mathrm{RED}}}{\rho_{\mathrm{NIR}} + 6\rho_{\mathrm{RED}} - 7.5\rho_{\mathrm{BLUE}} + 1}, \tag{4}$$

where ρ_{NIR}, ρ_{RED}, and ρ_{BLUE} are the surface reflectance of MODIS bands, and the coefficients adopted in the EVI algorithm are defined to correct for the canopy background adjustment and the aerosol influences.[11,36]

The following VCI_{evi} equation was applied on the final EVI database:

$$VCI_{evi} = \frac{EVI_i - EVI_{min}}{EVI_{max} - EVI_{min}}.$$

Here, VCI_{evi} is the vegetation condition index model constructed by the EVI time series (2012 to 2016), EVI_i is the current synthesized EVI of the 8 days, and EVI_{max} and EVI_{min} represent the maximum and minimum EVI value of each pixel in the database during the period from 2012 to 2016, respectively.

3.2.4 *Normalized difference moisture index*

The NDMI has a high correlation with wetness and has been shown to be a promising technique for monitoring.[37] NDMI is based on the contrast between midinfrared (MIR) and nearinfrared (NIR) reflectance, which are sensitive to changes in vegetation leaf structure and water content.[38–40] The equation used to calculate the NDMI is as follows:

$$NDMI = \frac{\rho_{NIR} - \rho_{MIR}}{\rho_{NIR} + \rho_{MIR}}, \tag{5}$$

where ρ_{NIR} and ρ_{MIR} are the surface reflectance in the NIR and MIR of the MODIS bands, respectively.

3.2.5 *Vegetation supply water index*

If drought occurs, the water supply of a crop is deficient, crop growth is affected, and the vegetation index (NDVI) will decrease. A crop without enough water is forced to close stomata, which causes the canopy temperature of the crop to rise.[14] Based on this principle, previous studies have defined the VSWI as follows:

$$VSWI = T_c/NDVI, \tag{6}$$

where T_c is the vegetation canopy temperature, represented in this paper by data of Terra MODIS (MOD11A2, where T_c is approximated by the daytime radiometric temperature, T_s or LST_{day}), and the NDVI is calculated according to Eq. (3).

3.2.6 *Temperature vegetation dryness index*

The TVDI has been widely applied as an indicator to estimate soil moisture based on empirical interpretation of the NDVI-LST triangle.[41] In the NDVI-LST space, the upper sloping edge of the triangle is defined as the dry edge and the lower sloping edge is defined as the wet edge, with both representing extreme conditions of soil moisture and evapotranspiration. TVDI is calculated by rescaling the radiometric surface temperature observed at each pixel as LST_{obs} between LST_{dry} and LST_{wet} values, defined for different levels of NDVI according to

$$TVDI = \frac{LST_{obs} - LST_{wet}}{LST_{dry} - LST_{wet}}, \tag{7}$$

where LST_{obs} is the observed LST at the pixel, LST_{wet} is the minimum LST for wet pixels as a given NDVI interval, and LST_{dry} is the maximum LST for dry pixels.

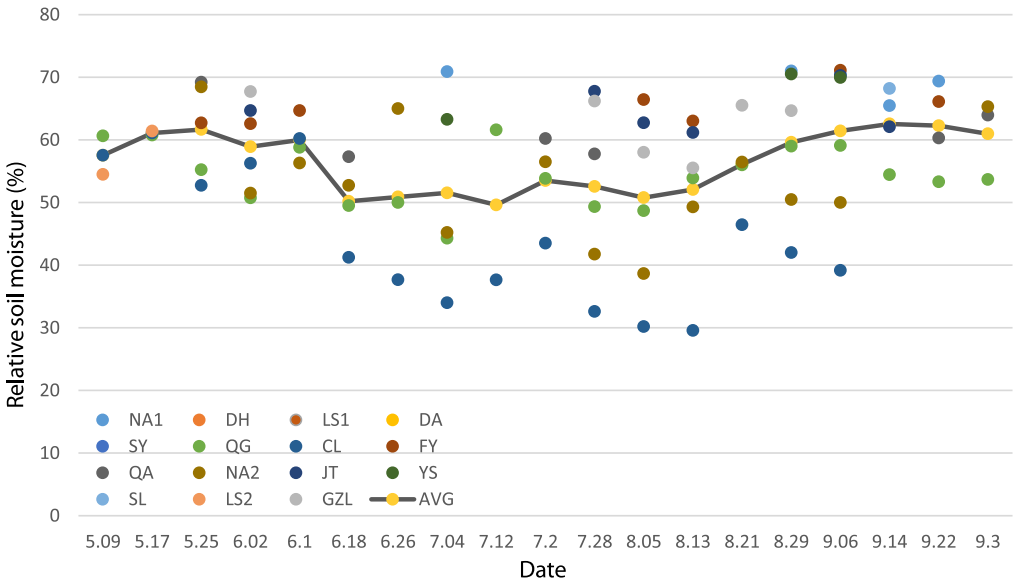

Fig. 2 Time series of RSM (%) at a depth of 10 cm at each station (for station details, see Table 2).

4 Results and Discussion

4.1 *Observations of Soil Moisture During the Whole Growth Period*

In this case, soil moisture data (relative soil moisture or RSM) is the ratio of the soil moisture content to the field soil water retention capacity, representing the ground truth observation. There are often droughts with RSM $< 60\%$. We built a time series of RSM at a depth of 10 cm in each station to more clearly show the process of drought and the changes in soil moisture (Fig. 2). To compare the performances of various drought indices, we used a linear regression model between the indices and the RSM. These results show that there was no drought at the beginning of the growth season, followed by soil moisture decrease from June 18 to August 20 as a drought occurred and expanded, which was then mitigated at the end of the growth season. The values of average soil moisture show the occurrence, development, and mitigation of the drought process. In addition, the RSM data from the automated meteorological stations are credible, without outlier values as can be caused by soil cracking or the presence of a gap between the sensor and the soil.[42]

4.2 *Comparison of the Indices in Different Phenological Periods*

The correlation coefficient (r) of TVDI over an entire maize-growing season was relatively high compared to other indices between the beginning of June and the end of August, which indicates that TVDI is more sensitive to soil moisture variation across most of the maize-growing season (Fig. 3).

In the early stage of a maize growth season (May 9 to June 18), soil tends to be bare, with low vegetation cover.[43] Our results show that ATI, a well-known and more sensitive indicator for bare soil monitoring according to the theory of apparent soil thermal inertia,[44] is preferable to other indices during the early vegetative growth stage. These results are also consistent with a previous finding noting that the temperature difference should be larger than 10°C when the thermal inertia model is selected to derive soil moisture.[45]

In the middle stage of the maize growth season (June 26 to August 5), VCI_{ndvi}, VCI_{evi}, and NDMI tend to have an obvious advantage under high vegetation cover. In a study by Yagci et al.,[46] the VCI-based drought products were effective at detecting and monitoring agricultural drought in Texas, United States, and Europe. These indices can show the onset and

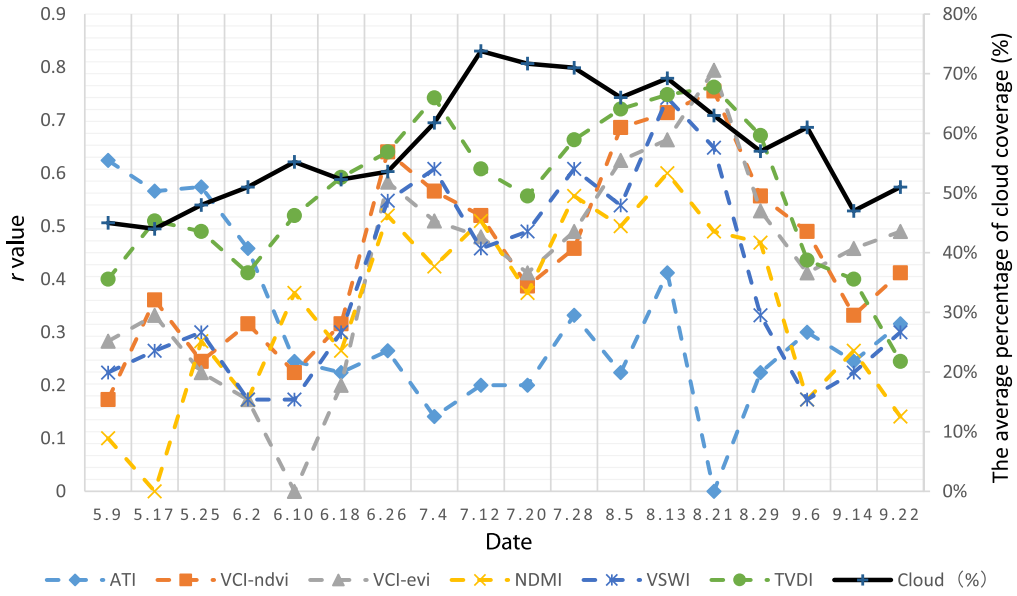

Fig. 3 Comparison of the correlation coefficent (*r* value) of each index and the average percentage of cloud cover (%) in the whole study area from May 9 to September 22.

spatial/temporal dynamics of agricultural droughts. However, in the case of China, a lower level of mechanization and a more complex planting structure yield abnormal minimum and maximum values, leading to inaccurate results. By introducing the parameter of land surface temperature or canopy temperature, VSWI and TVDI make up for this defect (VCI_{ndvi}, VCI_{evi}, and NDMI) and further improve the correlational relationship.[47] Chen et al.[48] retrieved surface soil moisture from MODIS TVDI and AMSR-E soil moisture data in the case of Taiwan, with the results showing positive correlation between TVDI and rainfall.

At the end of the maize-growing season (August 13 to September 22), VCI_{ndvi}, VCI_{evi}, and NDMI gradually lose the advantage with the natural decrease of vegetation coverage. ATI, VSWI, and TVDI showed the same trend.

From mid-June to mid-July and July 20 to August 21, these indices showed a positive relationship ($r_d = 0.514$) with relatively low soil moisture, higher than the average value ($r_a = 0.455$) across the whole growth season. This result shows that the indices are more sensitive to the drought process. Therefore, in order to compare the performance of the agricultural drought indices, further study should focus more on the process of drought by simulating the entire process of the occurrence, expansion, and mitigation of drought events.[49]

4.3 *Analysis of the Hysteresis and the Influence of Clouds*

On one hand, cloud cover is viewed as a parameter with uncertainty. Relatively lower correlation coefficients (r) of all the indices were observed under a higher percentage of cloud cover persisting from the beginning of June to the beginning of August (Fig. 3). Our findings suggest that an 8-day composite is required to avoid influences such as cloud cover and image noise.

4.4 *Comparing the Correlation Coefficient Among the Indices*

In order to show the difference of coefficients among the indices, we built a correlation coefficient matrix of indices to show their consistency with the description of agricultural drought (Table 3). The result shows that ATI and TDVI are much more independent than the others. Our findings suggest a necessity to classify the indices into three main types in order to avoid using methods with the same result.

Table 3 Matrix of r for the correlation coefficient among drought indices.

	ATI	VCI_{ndvi}	VCI_{evi}	NDMI	VSWI	TVDI
ATI	1					
VCI_{ndvi}	0.462	1				
VCI_{evi}	0.496	0.912	1			
NDMI	0.616	0.789	0.814	1		
VSWI	0.391	0.868	0.767	0.727	1	
TVDI	0.187	0.346	0.370	0.110	0.221	1

5 Conclusions

In this study, we performed a statistical evaluation comparing the performance of different drought indices, including ATI, VCI_{ndvi}, VCI_{evi}, NDMI, VSWI, and TVDI for agricultural drought in Songliao Plain, China. The results indicated the measured indices are useful in drought monitoring and can be used to track the drought process. On the other hand, we found hysteresis in time series, particularly in the mismatch between RSM data and MODIS data. In addition, data artifacts can affect and restrict monitoring accuracy. These include variability in planting patterns between individual farmers, which poses a challenge to remote sensing analyses at large spatial scales. Since each of the observed indices performed best under various circumstances, we suggest that it is necessary to choose the right index or multi-indices in order to support robust conclusions.

Acknowledgments

This work was supported by the NSFC Projects of International Cooperation and Exchanges (No. 61661136005), the CAMS Basic Research Funds-regular (No. 2018Z008), and National Nature Science Foundation of China (NSFC) (No. 41375117). The authors would like to thank the anonymous reviewers and the editors for their valuable comments and suggestions, and Editage (www.editage.com) for English language editing.

References

1. S. B. Fang, J. J Yang, and G. S. Zhou, "Change trend and distributive characteristics of agrometeorological disasters in China in recent 30 years," *J. Nat. Disasters* **5**, 69–73 (2011).
2. D. J. Li et al., "Identification of drought and drought hazard assessment in midwest of Jilin province based on SVDI," *Bull. Soil Water Conserv.* **37**(4), 321–326, 332 (2017).
3. D. Wu, J. J. Qu, and X. Hao, "Agricultural drought monitoring using MODIS-based drought indices over the USA Corn Belt," *Int. J. Remote Sens.* **36**(21), 5403–5425 (2015).
4. S. B. Fang, W. G. Yu, and Y. Qi, "Spectra and vegetation index variations in moss soil crust in different seasons, and in wet and dry conditions," *Int. J. Appl. Earth Obs. Geoinf.* **38**, 261–266 (2015).
5. B. Shen and S. B. Fang, "Vegetation coverage changes and their response to meteorological variables from year 2000 to 2009 in Naqu, Tibet, China," *Can. J. Remote Sens.* **40**(1), 67–74 (2014).
6. J. C. Price, "On the analysis of thermal infrared imagery: the limited utility of apparent thermal inertia," *Remote Sens. Environ.* **18**(1), 59–73 (1985).
7. F. N. Kogan, "Remote sensing of weather impacts on vegetation in non-homogeneous areas," *Int. J. Remote Sens.* **11**(8), 1405–1419 (1990).
8. C. J. Tucker, "Red and photographic infrared linear combinations for monitoring vegetation," *Remote Sens. Environ.* **8**(2), 127–150 (1979).

9. C. J. Tucker and B. J. Choudhury, "Satellite remote sensing of drought conditions," *Remote Sens. Environ.* **23**(2), 243–251 (1987).
10. L. Ji and A. J. Peters, "Assessing vegetation response to drought in the northern Great Plains using vegetation and drought indices," *Remote Sens. Environ.* **87**(1), 85–98 (2003).
11. A. Huete, C. Justice, and H. Liu, "Development of vegetation and soil indices for MODIS-EOS," *Remote Sens. Environ.* **49**(3), 224–234 (1994).
12. B. C. Gao, "NDWI—a normalized difference water index for remote sensing of vegetation liquid water from space," *Remote Sens. Environ.* **58**(3), 257–266 (1996).
13. E. H. Wilson and S. A. Sader, "Detection of forest harvest type using multiple dates of Landsat TM imagery," *Remote Sens. Environ.* **80**(3), 385–396 (2002).
14. T. N. Carlson, R. R. Gillies, and E. M. Perry, "A method to make use of thermal infrared temperature and NDVI measurements to infer surface soil water content and fractional vegetation cover," *Remote Sens. Rev.* **9**(1–2), 161–173 (1994).
15. I. Sandholt, K. Rasmussen, and J. Andersen, "A simple interpretation of the surface temperature/vegetation index space for assessment of surface moisture status," *Remote Sens. Environ.* **79**(2), 213–224 (2002).
16. T. Y. Chang et al., "Estimation of root zone soil moisture using apparent thermal inertia with MODIS imagery over a tropical catchment in Northern Thailand," *IEEE J. Sel. Top. Appl. Earth Obs. Remote Sens.* **5**(3), 752–761 (2012).
17. A. Maltese, F. Capodici, and G. Ciraolo, "Errata: mapping soil water content under sparse vegetation and changeable sky conditions: comparison of two thermal inertia approaches," *J. Appl. Remote Sens.* **7**(1), 073548 (2013).
18. W. T. Liu and F. N. Kogan, "Monitoring regional drought using the vegetation condition index," *Int. J. Remote Sens.* **17**(14), 2761–2782 (1996).
19. Q. Feng, G. L. Tian, and Q. H. Liu, "Research on the operational system of drought monitoring by remote sensing in China," *J. Remote Sens.* **7**(1), 14–18 (2003).
20. C. Wang et al., "Evaluating soil moisture status in China using the temperature vegetation dryness index (TVDI)," *Can. J. Remote Sens.* **30**(5), 671–679 (2014).
21. Y. Wang, S. Sha, and L. Zhang, "Comparison and application of drought monitoring remote sensing indices in the Hedong Area of Gansu, China," *J. Desert Res.* **35**(4), 1006–1014 (2015).
22. G. Caccamo et al., "Assessing the sensitivity of MODIS to monitor drought in high biomass ecosystems," *Remote Sens. Environ.* **115**(10), 2626–2639 (2011).
23. Y. Gu et al., "Evaluation of MODIS NDVI and NDWI for vegetation drought monitoring using Oklahoma Mesonet soil moisture data," *Geophys. Res. Lett.* **35**(22), 1092–1104 (2008).
24. J. Rhee, J. Im, and G. J. Carbone, "Monitoring agricultural drought for arid and humid regions using multi-sensor remote sensing data," *Remote Sens. Environ.* **114**(12), 2875–2887 (2010).
25. Y. Bayarjargal et al., "A comparative study of NOAA–AVHRR derived drought indices using change vector analysis," *Remote Sens. Environ.* **105**(1), 9–22 (2006).
26. J. Zhang, "Risk assessment of drought diaster in the maize-growing region of Songliao Plain, China," *Agric. Ecosyst. Environ.* **102**(2), 133–153 (2004).
27. X. Yin et al., "Soil tillage practices coping with drought climate change in central region of Songliao Plain," *Trans. Chin. Soc. Agric. Eng.* **28**(22), 123–131 (2011).
28. https://lpdaac.usgs.gov
29. J. C. Price, "The potential of remotely sensed thermal infrared data to infer surface soil moisture and evaporation," *Water Resour. Res.* **16**(4), 787–795 (1980).
30. A. P. Cracknell and Y. Xue, "Thermal inertia determination from space—a tutorial review," *Int. J. Remote Sens.* **17**(3), 431–461 (1996).
31. J. A. Sobrino and M. H. El Kharraz, "Combining afternoon and morning NOAA satellites for thermal inertia estimation: 1. Algorithm and its testing with hydrologic atmospheric pilot experiment-Sahel data," *J. Geophys. Res. Atmos.* **104**(D8), 9445–9453 (1999).
32. J. A. Sobrino and M. H. El Kharraz, "Combining afternoon and morning NOAA satellites for thermal inertia estimation: 2. Methodology and application," *J. Geophys. Res. Atmos.* **104**(D8), 9455–9465 (1999).

33. S. Liang, "Narrowband to broadband conversions of land surface albedo I: algorithms," *Remote Sens. Environ.* **76**(2), 213–238 (2001).
34. J. B. Campbell, *Introduction to Remote Sensing*, The Guilford Press, New York (1987).
35. F. N. Kogan, "Application of vegetation index and brightness temperature for drought detection," *Adv. Space Res.* **15**(11), 91–100 (1995).
36. A. Huete et al., "A comparison of vegetation indices over a global set of TM images for EOS-MODIS," *Remote Sens. Environ.* **59**(3), 440–451 (1997).
37. S. Jin and S. A. Sader, "MODIS time-series imagery for forest disturbance detection and quantification of patch size effects," *Remote Sens. Environ.* **99**(4), 462–470 (2005).
38. D. J. Hayes and W. B. Cohen, "Spatial, spectral and temporal patterns of tropical forest cover change as observed with multiple scales of optical satellite data," *Remote Sens. Environ.* **106**(1), 1–16 (2007).
39. N. R. Goodwin et al., "Estimation of insect infestation dynamics using a temporal sequence of Landsat data," *Remote Sens. Environ.* **112**(9), 3680–3689 (2008).
40. D. J. Hayes et al., "Estimating proportional change in forest cover as a continuous variable from multi-year MODIS data," *Remote Sens. Environ.* **112**(3), 735–749 (2008).
41. Z. Gao, W. Gao, and N. B. Chang, "Integrating temperature vegetation dryness index (TVDI) and regional water stress index (RWSI) for drought assessment with the aid of LANDSAT TM/ETM+ images," *Int. J. Appl. Earth Obs. Geoinf.* **13**(3), 495–503 (2011).
42. D. L. Wu, T. T. Gao, and H. X. Xue, "The study of quality control for observing data of automatic soil moisture," *Hans J. Soil Sci.* **04**(1), 1–10 (2016).
43. K. Song and Z. Wang, "Evapotranspiration estimation using moderate resolution imaging spectroradiometer products through a surface energy balance algorithm for land model in Songnen Plain, China," *J. Appl. Remote Sens.* **5**(1), 053535 (2011).
44. S. C. Yang et al., "Monitoring soil moisture by apparent thermal inertia method," *Chin. J. Eco-Agric.* **19**(5), 1157–1161 (2011).
45. G. Cai et al., "Soil moisture retrieval from MODIS data in Northern China Plain using thermal inertia model," *Int. J. Remote Sens.* **28**(16), 3567–3581 (2007).
46. A. L. Yagci et al., "Global agricultural drought mapping: results for the year 2011," in *IEEE Int. Geoscience and Remote Sensing Symp.* Vol. **53**, pp. 3764–3767 (2012).
47. M. E. Holzman, R. Rivas, and M. C. Piccolo, "Estimating soil moisture and the relationship with crop yield using surface temperature and vegetation index," *Int. J. Appl. Earth Obs. Geoinf.* **28**(5), 181–192 (2014).
48. C. F. Chen et al., "Retrieving surface soil moisture from Modis and Amsr-E Data: a case study in Taiwan," *ISPRS Int. Arch. Photogramm. Remote Sens. Spatial Inf. Sci.* **XXXIX-B3**, 379–383 (2012).
49. H. Sun, Y. H. Chen, and H. Q. Sun, "Comparisons and classification system of typical remote sensing indexes for agricultural drought," *Trans. Chin. Soc. Agric. Eng.* **28**(14), 147–154 (2012).

Yang Song received his master's degree in cartography and geographical information system from Liaoning Normal University, China. Currently, he is a PHD candidate in China Agricultural University. His current research focuses on the monitoring of drought based on remote sensing and GIS in arid and semiarid regions.

Biographies for the authors are not available.